Heat Transfer Efficiency and Capital Cost Evaluation of a Three-Phase Direct Contact Heat Exchanger for the Utilisation of Low-Grade Energy Sources

Hameed B. Mahood *[1, 2], Alasdair N. Campbell[1], Rex B. Thorpe[1], and Adel O. Sharif [1,3]

[1]Centre for Osmosis Research and Applications (CORA), Department Chemical and Process Engineering, Faculty of Engineering and Physical Sciences, University of Surrey, Guildford GU2 7XH, UK

*e-mail: h.al-muhammedawi@surrey.ac.uk

[2]University of Misan, Misan, Iraq, e-mail: hbmahood@yahoo.com

[3]The Qatar Foundation, Qatar Energy and Environment Research Institute, Qatar

Abstract

Low-grade energy cycles for power generation require efficient heat transfer equipment. Using a three-phase direct contact heat exchanger instead of a surface type exchanger, such as a shell and tube heat exchanger, potentially makes the process more efficient and economic. This is because of its ability to work with a very low temperature driving force, as well as its low cost of construction. In this study, an experimental investigation of the heat transfer efficiency, and hence cost, of a three-phase direct contact condenser has been carried out utilising a short Perspex tube of 70 cm total height and 4 cm internal diameter. Only 48 cm was used for the direct contact condensation. Pentane vapour with three different initial temperatures (40℃, 43.5℃ and 47.5℃) was contacted with water with an inlet temperature of 19℃. In line with previous studies, the ratio of the fluid flow rates was shown to have a controlling effect on the exchanger. Specifically, the heat transfer efficiency increased virtually linearly with this ratio, with higher efficiencies also being observed with higher flow

rates of the continuous phase. The effect of the initial temperature of the dispersed phase was shown to have a lower order impact than flow rate ratio. The capital cost of the direct contact condenser was estimated and it was found to be less than the corresponding surface condenser (shell and tube condenser) by 30 times. An optimum value of the continuous phase flow rate was observed at which the cost of the condenser is at a minimum.

Keywords: Three-phase direct contact condenser, heat transfer efficiency, costing

1. Introduction

Energy usage is increasing around the world due to the development of technologies and population growth. Recent research revealed that the demand for energy could rise by up to 1.7% annually until 2030 [1]. However, fossil fuels remain the dominant energy source, producing about 80% of the gross energy required, while renewable energy contributes only 11%. Accordingly, many environmental problems such as global warming, ozone depletion and air pollution will increase. Furthermore, the fossil fuel prices will likely rise. Hence, industrial waste energy, especially from low-grade heat sources, for power production has recently received more attention [1]. This can be efficiently achieved by using a direct contact concept.

Most popular heat exchangers that are used in practice are surface type heat exchangers, in which hot and cold fluids are separated completely by metallic barriers. Shell-and-tube heat exchangers are a classic example of this type of exchanger. This, of course, results in a reduction in the rate of heat exchange between fluids and consequently reduces the process's efficiency, and increases the capital and operational costs. As a result, the implementation of such heat exchangers in heat recovery processes, or in low-grade thermal energy cycles for power generation (e.g. in solar energy systems such as solar ponds and solar collectors), is inefficient.

Thus, attempts to enhance the efficiency of conventional heat exchangers have recently received more attention. For example, Dizaji et al. [2] have demonstrated experimentally that the effectiveness of a shell-coiled type heat exchanger is significantly improved by the injection of small air bubbles into the exchanger shell. In the same context, Rashidi et al. [3] studied theoretically the effect of using a porous material inside a conventional heat exchanger on its performance. Their exchanger was used for a solar energy application. They concluded that using a porous substrate with a high Darcy number can improve the thermal performance of the heat exchanger with an acceptable increase in pumping cost.

Alternatively, a direct contact heat exchanger allows working fluids to come into direct physical contact by eliminating the solid barriers. A high heat transfer rate, an absence of corrosion and fouling problems, a lower cost, a simple design and the potential to work at a very low temperature driving force are the main advantages of using direct contact heat exchangers. Accordingly, they can be found in many applications, for example water desalination, geothermal power generation, solar energy [4-6] and in low cost hydrogen generation from a direct mixing of water or gaseous hydrocarbons gas with Pb or Pb-Bi heavy liquid metal [7] . The three-phase direct contact heat exchanger (used as an evaporator or condenser) generally operates by injection of drops or bubbles as a dispersed phase into a flowing column of another immiscible liquid, which acts as a continuous phase. The temperature of the continuous phase must be above the boiling point of the drops for evaporation, or less than the saturation temperature of the bubbles in the case of condensation. An intimate mixing of the dispersed phase and the continuous phase can be achieved. The drops or bubbles therefore evaporate or condense directly when they touch the continuous phase, and two-phase bubbles are formed.

The main limitation of the direct contact heat exchanger is that a mutual mixing of fluids occurs due to their intimate direct contact. This necessitates an additional cost for separation.

Practically, this problem can be all but eliminated by using two immiscible fluids, separation of which can be achieved using gravity. A second, more problematic, limitation is the difficulty in accurately predicting the direct contact heat exchanger's performance. Due to the mixing of the two fluids, a high, but difficult to predict, interfacial area for heat exchange is created, especially when the process involves bubbles or drops [8]. The difficulty in modelling the extent of this interfacial area means there is a general dearth of specialised mathematical theory and, indeed, experimental measurements or correlations, which can be used for design proposes. This is especially true for condensers. Furthermore, a detailed understanding of the hydrodynamic phenomena is also required if a functional, plant-scale exchanger is to be designed. Such direct contact devices can, potentially, suffer from problems due to flooding and back mixing. Such problems can only be understood, and ultimately overcome, through detailed experimental and theoretical study.

In spite of the great potential of the direct contact heat exchanger for use in fields such as energy recovery and renewable energy it is, somewhat surprisingly [8, 9], not widely mentioned in the heat transfer handbooks. Much attention has focussed on the simpler problem of the heat transfer and the hydrodynamics in the direct contact condensation of single bubbles [5, 6, 10-18] and trains of multiple bubbles [20-22]. Only Sideman and Moalem [23] studied, theoretically, the parameters that control the performance of a direct contact three-phase condenser. They exploited previous models of the condensation of a single two-phase bubble in an immiscible liquid. Recently, Mahood et al. investigated the three-phase direct contact condenser theoretically [21] and experimentally [24-29]. These studies investigated various characteristics of the thermal performance of a lab.-scale direct contact condenser during both transient and steady state operation. Specifically, the overall volumetric heat transfer coefficient during transient operation [24] was measured. A model was proposed for the steady state temperature distribution, which compared favourably with

the experimental measurements [25]. Furthermore, a model predicting the transient temperature profile along the length of the direct contact column was also developed [26]. The effects of various parameters, such as the ratio of the mass flow rates of the continuous and dispersed phases, on the outlet temperatures was also investigated [27]. In addition, the variation of the volumetric heat transfer along the column [28], and the suitability of direct contact condensation for use in desalination were also investigated [29].

These studies produced promising results, which showed the effect of key process parameters on the thermal outputs of the condenser. The specifics of these thermal effects must, however, be considered in totality by investigating the condenser's efficiency and capital cost; it is these parameters that will ultimately determine the industrial relevance of this technology. These two critical measures of exchanger performance have not been investigated previously. Therefore, this work reports these important properties of the three-phase direct contact condenser for the first time.

Specifically, an experimental investigation of the heat transfer efficiency in a three-phase direct contact is described in section 2. The effects of the operational parameters, such as the dispersed phase mass flow rate, the continuous phase mass flow rate and the initial dispersed phase temperature on the heat transfer efficiency are examined in section 3. Subsequently, these results are used to estimate the capital cost of the direct contact condenser, which is then compared to the cost of a traditional shell and tube condenser.

2. Experimental setup and procedure

A general view and a schematic layout of the experimental test rig are shown in Fig. 1(a). The test section is a Perspex cylindrical column with a total height of 70 cm and 4 cm internal diameter. The volume is thus 0.00352 m^3. Only 48 cm (0.00241 m^3) was used as the active height (i.e. the height containing the continuous phase) during the experiments. The pentane,

in the vapour phase, was introduced into the bottom of the column via a tube of 6mm internal diameter. Similarly, the continuous phase was removed from the bottom of the column via a tube with 6 mm internal diameter. At the top of the column, a 6 mm tube introduced the continuous phase, and a 6 mm tube, well above the initial water level, was used to remove the condensed pentane. In addition, five equally spaced (12 cm spacing) holes along the height of the column were used to insert thermocouples into the column to measure the temperature of the continuous phase and the condensed material.

The heating vessel is a rectangular stainless steel vessel, of dimensions $50\ \text{cm} \times 40\ \text{cm} \times 50\ \text{cm}$ ($0.1\ \text{m}^3$ volume). Two electrical heaters are fixed near to its base; each one has a power of 3kW, and is connected to a thermostatic controller. The vessel contains a long copper coil (6.5 m long with 6 mm diameter) which can be completely immersed in water, which is used as a heating medium. The temperature of this water was measured by a digital thermometer. This coil was used to carry and vaporise the dispersed phase pentane. At the base of the vessel, the coil connects to the liquid pentane storage tank, whilst at the top of the vessel the coil joins with the condenser's test section via an externally heated short tube and sparger. The sparger is a conical shape, formed from Perspex with a circular plate attached to its top. The total diameter of the sparger at the injection point is 34 mm and the sparger plate diameter is 26 mm. The total height of the sparger is 42 mm. The plate contains 48 orifices each of 0.5 mm diameter, and is fixed to the body of the sparger by 8 screws. The orifice plate has a thickness of 3 mm. Eight radially aligned rows of 4 orifices appear in the pattern shown in Fig. 1 (b). Additionally, two holes were added circumferentially in between the rows.

The water supply system provides the continuous phase in the condenser. The water storage tank is a large plastic rectangular shape tank with a volume of 160 L. A low flow rate centrifugal pump (4 kg/min maximum mass flow rate) feeds the continuous phase from the

storage tank to the top of the condenser via a rotameter. The water flow was controlled manually by a recirculation loop.

The liquid pentane storage tank is a 10 L plastic tank connected to the liquid pentane feed pump via a short plastic tube. The pump is a centrifugal low flow rate pump (4 kg/min maximum) which supplies pentane to the heating vessel. A recirculation loop controlled the mass flow rate of liquid pentane. A pressure gauge (1 barg maximum) measured the liquid pentane feed pressure, before it entered the heating vessel. In addition, the temperature and pressure of the vapour pentane were measured before injection into the test section of the condenser. This technique is described in more detail elsewhere [30] and was used in previous studies [24-28]. The pentane was injected at a pressure of 0.2 barg. A large temperature range trace heater (total power 10 W/m^2 and a maximum working temperature of 200℃) with controller maintained a constant vapour temperature in the line prior to injection. The vapour temperature was measured just before injection into the test section by a thermocouple. Calibrated K-Type thermocouples measured (i) the temperature of the continuous phase along the test section, (ii) the dispersed phase vapour, (iii) the condensate and (iv) the continuous phase inlet and outlet. All these thermocouples connect to an eight channel data logger and PC.

Normal Pentane (C_5H_{12}) (Fisher Scientific, 99+ % purity) was used as the dispersed phase; its general and physical properties are given in Table 1. Tap water was used as the continuous phase. The experiments began with the preparation of the continuous phase by heating the water to 19℃. The large storage tank size and short duration (2-3 minutes) of each individual experimental run helped to maintain the continuous phase temperature at this value. The inlet and outlet rotameters were set such that the flow rates of water into and out of the column were identical. Concomitantly, the heating vessel was warmed by gradually increasing the electrical power to the heaters until the desired temperature for the particular experiment was

reached. The liquid pentane was then vaporised in the coil, and injected into the direct contact test section via the trace-heated pipe. The injection pressure and the vapour temperature were measured using a pressure gauge and a thermocouple. At the point of vapour injection, the temperature distribution along the direct contact test section (condenser) was measured and read by the PC. The condensate formed (as a separated layer at the top of the column) well above the water inlet, and after each run it was collected and sent back to the liquid pentane storage tank, or stored and used in another run. The condenser was run for around 3 minutes until a steady state was reached in the column. A separating conical flask was used for separating the condensed pentane from any entrained water. The dispersed phase mass flow rate was calculated using a mass balance for each individual run i.e. the collected pentane was weighed and divided by the run duration. The initial conditions of the experiments appear in Table 2. The uncertainty in the thermocouples appears in Tables 3. The uncertainty of the continuous flow measurement depends on flow rate range. It was $\pm 6.0\%$ for flow rates from 0 to $0.1 kg/min$, $\pm 9.7\%$ for flows from $0.1 kg/min$ to $0.3 kg/min$ and finally $\pm 4.7\%$ for continuous phase flow rates greater than $0.3 kg/min$. For the dispersed phase mass flow rate measurement, the mass balance after each run was used. The total error in the measurements, which consisted of the error in the digital scale, the loss of condensate due to the miscibility of pentane in water (which is very small), the time of the run and the possibility of draining the condensate with the continuous phase was calculated. The inaccuracy of the dispersed phase mass flow rate is estimated at $\pm 11\%$.

Table 1 The physical properties of n-pentane at 1 bar and saturation temperature

Property	Values
Saturation temperature ($°C$)	36.0
Molar mass ($kg/kmol$)	72.15
Thermal diffusivity (m^2/s)	7.953×10^{-8}

Specific heat of liquid $(\boldsymbol{kJ/kg\ K})$	2.363
Specific heat of vapour $(\boldsymbol{kJ/kg\ K})$	1.66
Thermal conductivity of liquid $\boldsymbol{W/m\ K}$	0.1136
Thermal conductivity of vapour$(\boldsymbol{W/m\ K})$	0.015
Kinematic viscosity $(\boldsymbol{m^2/s})$	2.87×10^{-7}
Viscosity $(\boldsymbol{kg/m\ s})$	1.735×10^{-4}
Latent heat of vaporisation $(\boldsymbol{kJ/kg})$	359.1
Density of liquid $(\boldsymbol{kg/m^3})$	621
Density of vapour $(\boldsymbol{kg/m^3})$	2.89
Surface tension $(\boldsymbol{N/m})$	0.01432

Table 2 The initial conditions of the experiments.

T_{vi}(℃)	T_{ci}(℃)	$H_o(m)$	$\dot{m}_c\left(\frac{kg}{min}\right)$	$R=\frac{\dot{m}_v}{\dot{m}_c}\times 100\%$				
40	19	0.48	***0.0564***	16.134	31.028	49.64	58.51	66.595
			0.107	11.186	13.983	18.178	22.373	32.628
			0.2015	7.318	9.922	13.693	14.883	19.051
			0.286	5.3497	7.447	8.95	10.56	14.335
			0.38	4.8	6.037	7.427	8.46	9.366
43.5	19	0.4	***0.0564***	15.319	11.49	8.13	4.825	3.935
			0.107	29.078	17.34	9.37	7.52	4.5
			0.2015	37.234	25.58	11.41	8.82	5.07
			0.286	41.666	26.7	14.25	10.489	6.776
			0.38	52.766	29.94	18.6	13.986	8.366
47.5	19	0.48	***0.0564***	3.89	5.674	7.674	11.281	13.222
			0.107	4.73	8.664	9.535	11.643	12.587
			0.2015	7.918	10.567	15.628	17.711	19.3
			0.286	11.606	16.92	22.876	26.708	28.582
			0.38	25.37	30.32	35.561	45.266	54.415

Table 3 Inaccuracy of the thermocouples

T(℃)	**Inaccuracy %**
T_{c1}	±0.440
T_{c2}	±0.508
T_{c3}	±0.325
T_{c4}	±0.359
T_{cond}	±0.582
T_{di}	±0.480
T_{ci}	±0.353

1

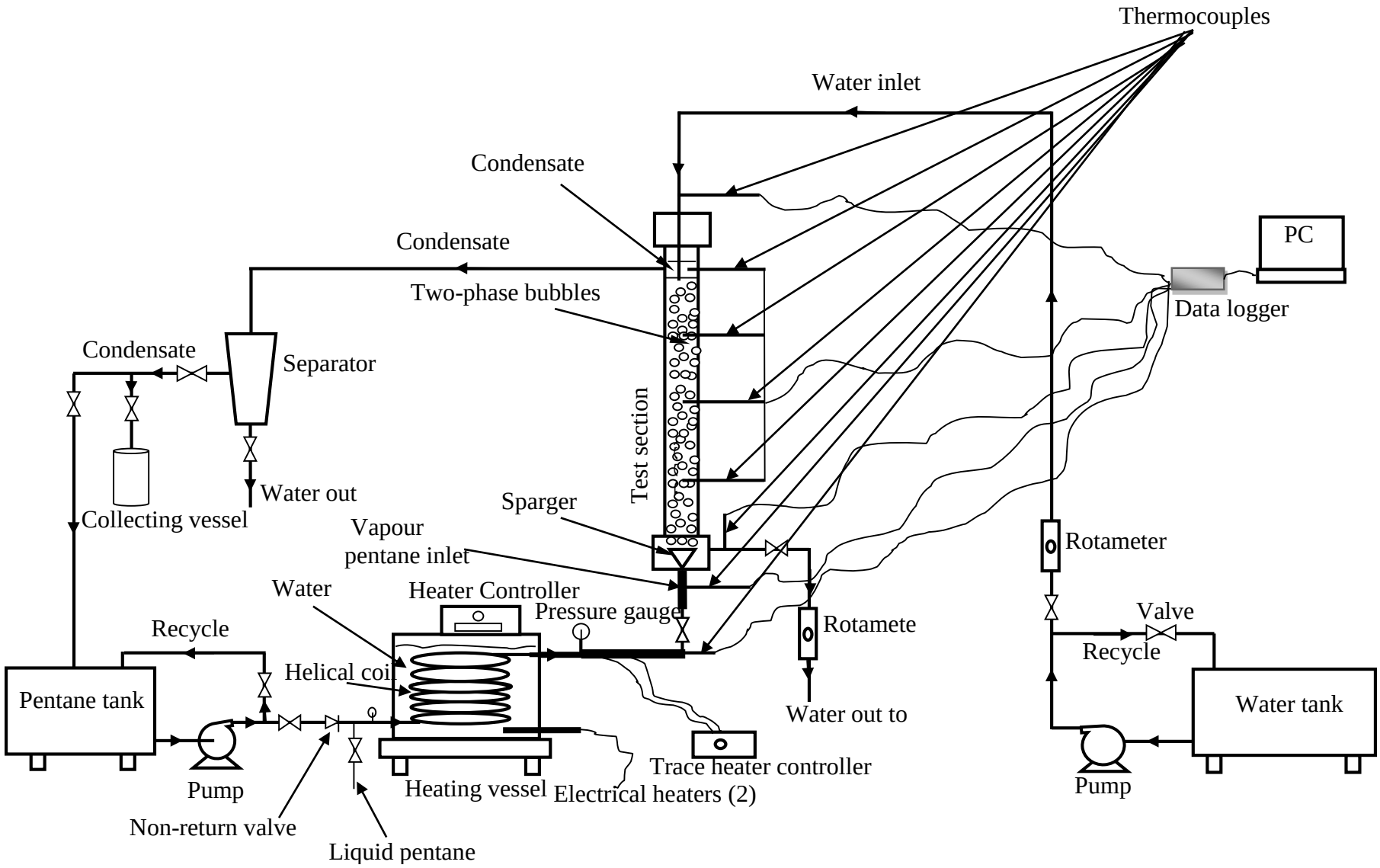

Fig. 1 a. Schematic diagram of the experimental rig.

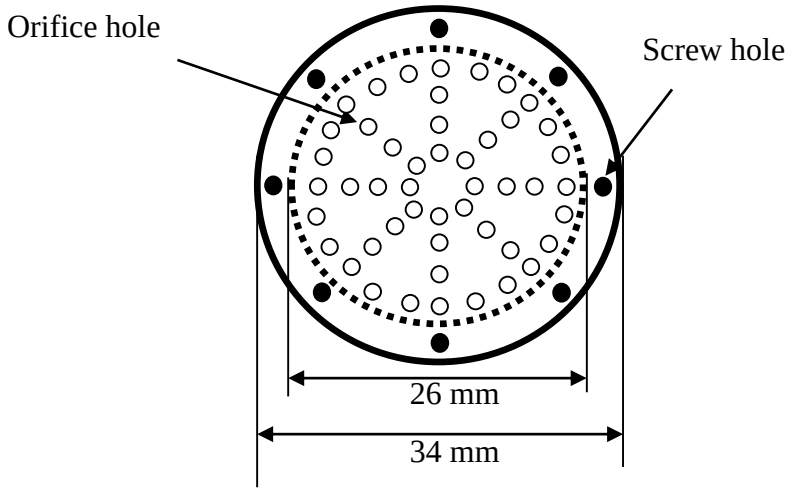

Fig. 1 b. Orifice plate configuration of the sparger.

3. Results and discussion

3.1 Heat Transfer Efficiency

The direct contact heat exchanger can save money, energy, and space because of its ability to transfer heat between contacting fluids efficiently, due to the absence of heat transfer surfaces. The efficient implementation of the three-phase direct contact condenser requires a good knowledge of the impact of different operational parameters on the exchanger performance.

Essentially, the direct contact condensation process is accomplished by mixing of the vapour with a subcooled liquid. A simple heat balance can be used to determine the amount of vapour condensed by a specific amount of liquid. Theoretically, the cooling fluid can be heated to any

desired temperature by controlling the pressure of the vapour and the liquid flow rates. The following expression is used to calculate the three-phase direct contact efficiency:

$$efficiency\ \% = \frac{T_{co}-T_{ci}}{T_{d,sat}-T_{ci}} \times 100\% \quad (1)$$

where T_{co}, T_{ci} and $T_{d,sat}$ represent the continuous phase outlet temperature, the continuous phase inlet temperature and the vapour saturation temperature, respectively. This, of course, assumes that no heat is lost to the surroundings. Given the short duration of the experiments, and the small temperature difference across the insulating Perspex wall of the column, this assumption is entirely reasonable in the current context.

The mass flow rate ratio has been shown to be an effective operational parameter for controlling the heat transfer characteristics of the three-phase direct contact condenser [25, 26]. The effect of the mass flow rate ratio, for three different initial dispersed phase temperatures, on the efficiency of the direct contact condenser is shown in Figs. 2-4. The mass flow rate ratio was altered by varying the dispersed phase mass flow rate with a constant continuous mass flow rate. As shown in Figs. 2-4 , the efficiency of the direct contact condenser increases with increasing mass flow rate ratio. For example, in Fig. 2, for an initial dispersed phase temperature of 40 °C it is clear that for each discrete value of continuous phase flow rate the efficiency increases almost linearly with mass flow rate ratio. It is also evident that the rate at which the efficiency increases with increased mass flow rate ratio depends on the continuous phase flow rate. Thus, at the highest continuous phase flow rate (0.38 kg/min) the efficiency increases above 50% when the mass flow rate ratio is approximately 59%. In contrast, at the lowest flow rate, the efficiency reaches this level when R ~ 12%. Unsurprisingly, the system is much more sensitive to variation in R when the continuous phase flow rate is low. This makes intuitive sense, as there is less cooling available via the continuous phase. Similar trends are evident in Figs. 3 and 4 for different initial temperatures of the dispersed phase. Comparison of all three plots also reveals that

there is a slight increase in efficiency when a higher initial temperature is used. This effect is, however, clearly second order when compared to the effect of mass flow rate ratio. As discussed above, the key factor determining the efficiency is the energy gained by the cold fluid ($T_{co} - T_{ci}$) with increasing mass flow rate ratio, which was noted and discussed by Mahood et al. [25]. Physically, the increase of the mass flow rate ratio means that more heating medium is supplied to the condenser, which results in an enhancement of the heat transfer process, and consequently an increase in the efficiency of the three-phase direct contact condenser. Interestingly, and depending somewhat on the continuous phase mass flow, the dispersed phase mass flow rate required to approach a relatively high efficiency seems low. This is, of course, impacts the operational cost of the three-phase direct condenser, because the process will be carried out using a relatively small quantity of working fluid.

The results presented above would suggest that the maximum efficiency can be achieved by using a low continuous phase mass flow rate and a high mass flow rate ratio; however, flooding is still the main shortcoming associated with the three-phase direct contact condenser. The probability of flooding actually increases with increasing dispersed phase mass flow rate, or decreasing continuous mass flow rate, i.e. when the mass flow ratio is large. This clearly places an operational limit on the mass flow ratio that can be practically employed, which compromises the efficiency somewhat. As with many engineering systems, a compromise between these competing effects must be sought. To reduce or avoid the negative effects of flooding, operation with a relatively high continuous phase mass flow rate is required. Figs. 2-4 clearly show that operating in this manner leads to a reduction in the efficiency of the condenser, but this can be offset by manipulation of the flow ratio and initial temperature of the dispersed phase. The three-phase direct contact condenser therefore can be operated more efficiently than the corresponding shell and tube condenser. As shown in Figs. 2-4 and for a constant mass flow rate ratio, a higher continuous phase mass flow rate results in

higher direct contact condenser efficiency. This could be due to an efficient condensation process taking place when sufficient cooling water is available; otherwise, a fraction of vapour is still not completely condensed. In the present study, these effects clearly appear at low continuous mass flow rates (0.06 to 0.11 kg/min). They gradually decrease with increasing continuous phase mass flow rate (0.11 - 0.20 kg/min) and nearly disappear at high continuous mass flow rates (0.20 - 0.38 kg/min). Practically, for a given dispersed phase mass flow rate, there is a continuous phase mass flow rate that is required to achieve a complete direct contact condensation process. The additional coolant in the condenser results in a reduction in the continuous phase outlet temperature, and subsequently, a reduction in the efficiency of the three-phase direct contact condenser.

Figure 5 shows the variation of the three-phase direct contact condenser efficiency with the temperature difference between the two-phases at their inlet conditions, for three different continuous mass flow rates. A slight increase of the condenser efficiency with increasing initial temperature difference between the contacting fluids is shown. A higher initial temperature difference between the contacting fluids results in a higher convective heat exchange, and increases the energy absorbed by the continuous phase. Again, it is quite clear that at a given temperature difference, the efficiency of the direct contact condenser is higher when the continuous mass flow rate is high. The error in the efficiency, which appears as error bars in the Fig. (2-4) was estimated using a similar method to that outlined elsewhere [31].

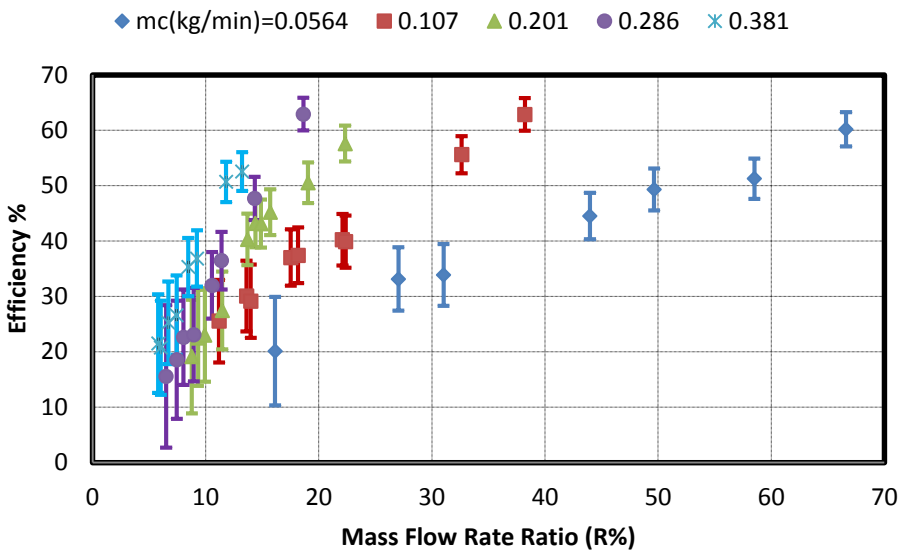

Fig. 2. Direct contact heat exchanger efficiency versus mass flow rate ratio for an initial dispersed phase temperature of 40 °C and five continuous phase flow rates

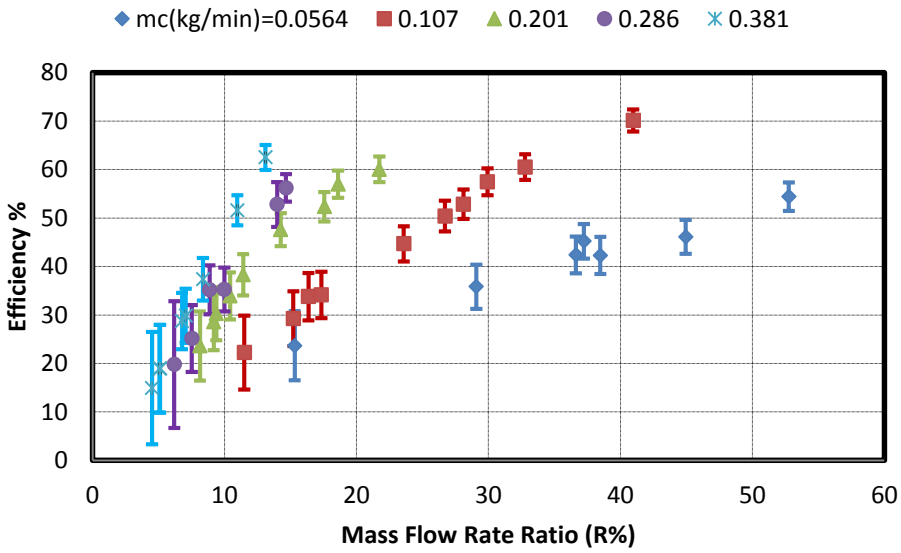

Fig. 3. Direct contact heat exchanger efficiency versus mass flow rate ratio for a dispersed phase initial temperature of 43.5 °C and five continuous phase flow rates

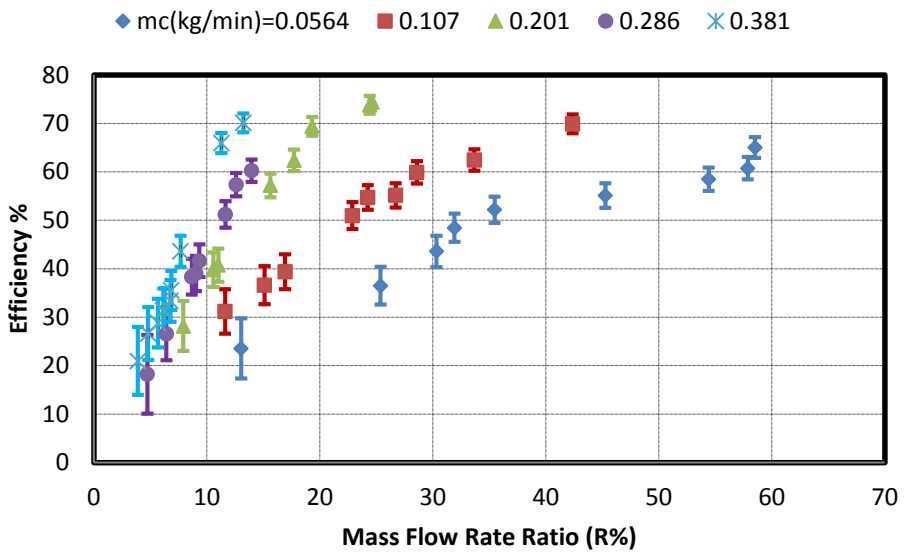

296

297 **Fig. 4.** Direct contact heat exchanger efficiency versus mass flow rate ratio for a dispersed
298 phase initial temperature of 47.5 °C and five continuous phase flow rates

299

300

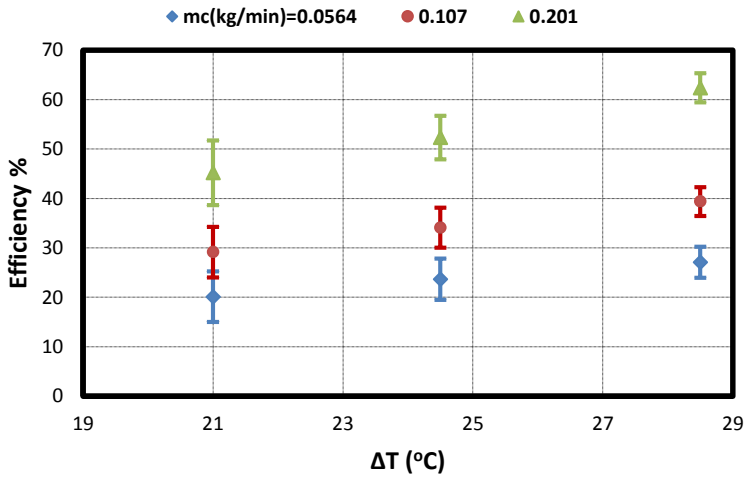

301

302 **Fig. 5.** Direct contact heat exchanger efficiency versus temperature difference between the
303 two-phases at $(T_{di} - T_{ci})$ for three different continuous mass flow rates

304

305

306

3.2 Direct contact condenser costing

Beside the limitations of thermal energy extraction, the costs, both initial and operational, are another problem encountered in the selection and use of the surface type heat exchanger. The high initial cost results from the large surface area required to overcome the low heat transfer rate, while the operational cost is mainly due to the expenses from the continuous maintenance due to fouling and corrosion. Although such problems can be alleviated by different technologies, an increase in capital and operational cost would result. For example, implementation of special materials of construction, which are normally expensive, increases the capital cost, and further treatment of feed water using e.g. corrosion inhibiters increases the operational cost. Therefore, the direct contact heat exchanger may be used, potentially, in fields when surface type heat exchangers are not economical. However, estimation of the capital cost of a direct contact condenser and comparison with the cost of shell and tube type of equivalent duty is very important to support this claim.

The cost of the three-phase direct contact condenser is estimated by exploiting the expression used for costing a pressure vessel. This is because the direct contact bubble type or spray column condenser largely consists of a pressure vessel. In this context, Guthrie [32] has suggested the following formula, based on the vessel size (height and diameter):

$$Cost\ (\$) = \left(\frac{M\&S}{280}\right)(101.9D^{1.066}H^{0.82}F_c) \quad (2)$$

where $M\&S$, D, H and F_c denote the Marshall and Swift cost index, the column diameter, the column height and the correction factor, respectively. The correction factor, F_c, depends on the column's operational pressure and its material of construction, and it is given by:

$$F_c = F_p F_m \quad (3)$$

For the purpose of comparison, a case is chosen where the column operates at atmospheric pressure and is made from carbon steel. Here, $F_c = 1$ [32].

The Six-Tenths Rule is used for pricing the shell and tube heat exchanger [33]. According to this rule, the cost of new equipment can be estimated if the cost of similar equipment, but for a different size, is available. The Six-Tenths Rule is given by:

$$C_A = C_B \left(\frac{Size\ A}{Size\ B}\right)^{0.6} \quad (4)$$

where C_A is the cost of new equipment (e.g. shell and tube heat exchanger) of size A, while C_B represents the cost of equipment of another size, B.

To update the shell and tube heat exchanger cost, the following expression is used [34]:

$$C_{A-new} = C_{A-old} \left(\frac{I_{A-new}}{I_{A-old}}\right) \quad (5)$$

where I represents the cost index, in our case the Marshall and Swift index.

Thus, the cost of chemical engineering equipment, including heat exchangers is directly proportional to its size (heat transfer area) raised to the power 0.6. The heat transfer area can be calculated as:

$$A = \frac{Q}{U\Delta T_{lm}} \quad (6)$$

where Q, U and ΔT_{lm} represent the heat transfer rate, the heat transfer coefficient and the log mean temperature difference, respectively. The log mean temperature difference may be calculated from the experimentally measured temperatures.

Accordingly, the heat exchanger cost can be written as:

$$cost = \left(\frac{Q}{U\Delta T_{lm}}\right)^{0.6} . K_c \quad (7)$$

The merit of the three-phase direct contact heat exchanger is its capability to offer a high heat transfer coefficient and therefore, a low area and low cost. One way to compare the performance of two different types of heat exchangers is to compare the heat transfer

coefficient (U) values. However, U is unbounded. The reciprocal of the heat transfer coefficient $(1/U)$ is another comparison, being the resistance to heat transfer, and for an improved design this should lie between the existing design value and zero. This is also convenient for graphical comparison. Hence, it is useful to rearrange Eq. (7) as:

$$\frac{Cost^{1/0.6}\Delta T_{lm}}{Q} = \frac{1}{U} \tag{8}$$

The cost index in equation 8 is plotted in Fig. 6 as a function of the flow rates of the continuous and dispersed phases. As shown in the figure, the capital cost of the three-phase direct contact condenser decreases with an increase in the dispersed phase mass flow rate, irrespective of the continuous phase flow rate. This is of course unsurprising given that an increase in the dispersed phase flow results in an increase in the mass flow ratio. As shown above, this results in an increase in the efficiency of the heat transfer. No, or very little, effect of the continuous phase mass flow rate on the capital cost can be seen in the figure, particularly if the error estimates are considered.

Figures 7-9 show the comparison between the capital cost of the three-phase direct contact condenser and a shell and tube condenser performing the same duty. It is clear that the capital cost of the shell and tube heat exchanger is largely independent of the dispersed phase mass flow rate. Therefore, regardless of the continuous phase mass flow rate, a large difference in capital cost between the two condensers is achieved at a high dispersed phase mass flow rate. These plots also highlight the significant potential savings that can be made by using a direct contact device. Indeed, the capital costs are lower by at least a factor of 5, but in many cases by an order of magnitude.

The effect of the continuous phase mass flow rate on the direct contact condenser's cost is shown in Figs. 10-12 for four different dispersed phase flow rates and three initial temperatures of the dispersed phase. It is clear that the condenser cost initially decreases as

the continuous phase mass flow rate is increased. It reaches a minimum value, the magnitude and location of which depends on the dispersed phase mass flow rate. Beyond the minimum value, the cost increases once more as the continuous flow rate is increased. This optimum value for the continuous phase clearly arises from the need to have sufficient continuous fluid to fully condense the dispersed phase, without having too much, which would impair the efficiency and therefore lead to an oversized exchanger.

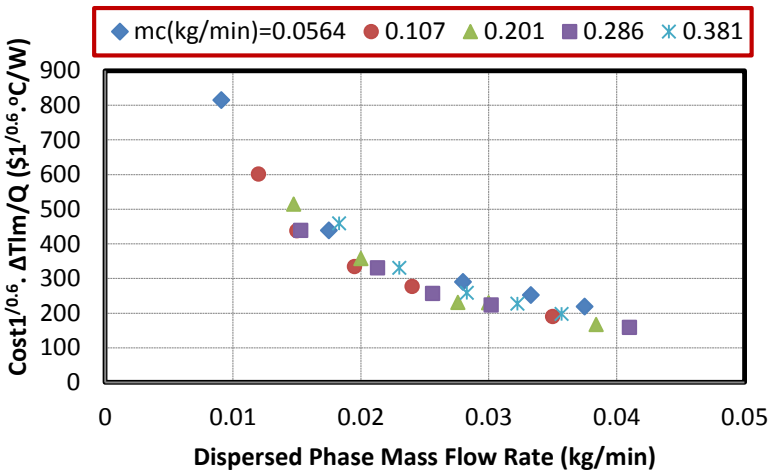

Fig. 6. The variation of capital cost of the three-phase direct contact condenser with the dispersed phase mass flow rate for a constant dispersed phase initial temperature (T_{di} = 40°C) and five different continuous phase mass flow rates.

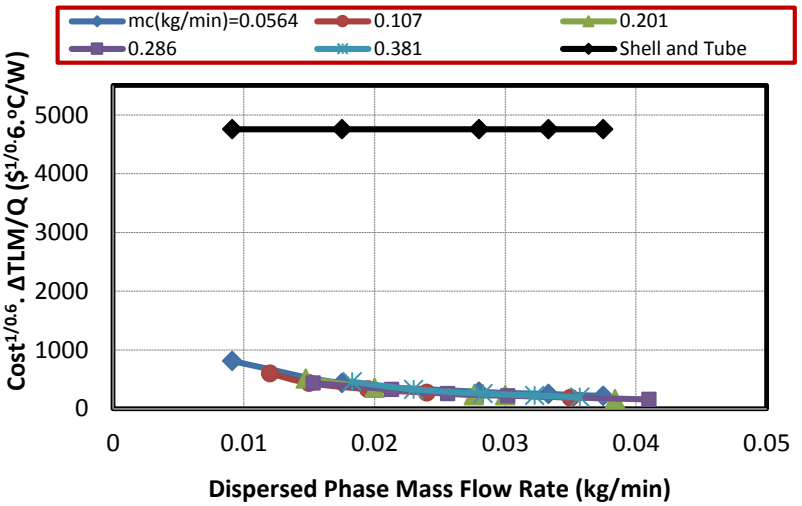

390

391 **Fig. 7.** Comparison between the three-phase direct contact condenser's capital cost and shell
392 and tube condenser cost for five different continuous phase mass flow rates and dispersed
393 phase initial temperatures (T_{di} = 40°C).

394

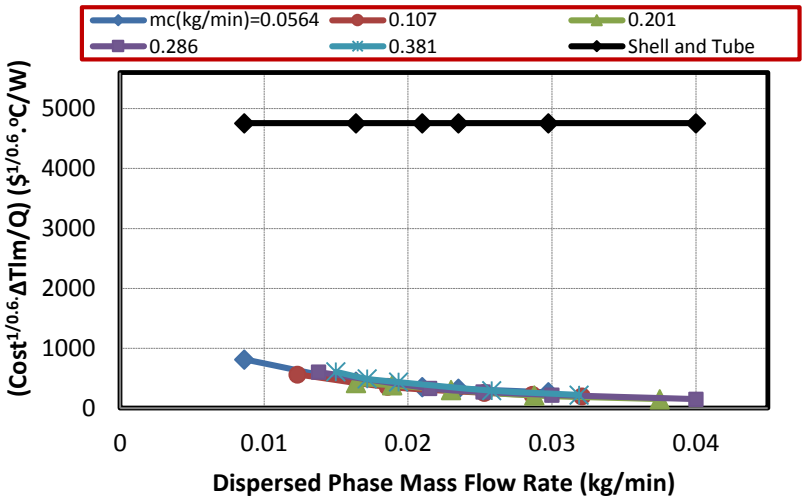

395

396 **Fig. 8.** Comparison between the three-phase direct contact condenser's capital cost and shell
397 and tube condenser cost for five different continuous phase mass flow rates and dispersed
398 phase initial temperatures (T_{di} = 43.5°C).

399

400

401

402

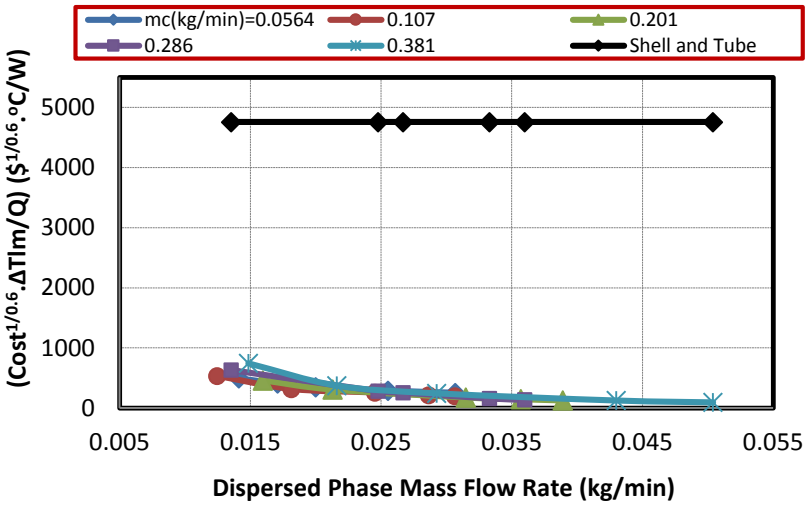

Fig. 9. Comparison between the three-phase direct contact condenser's capital cost and shell and tube condenser cost for five different continuous phase mass flow rates and dispersed phase initial temperatures (T_{di} = 47.5℃).

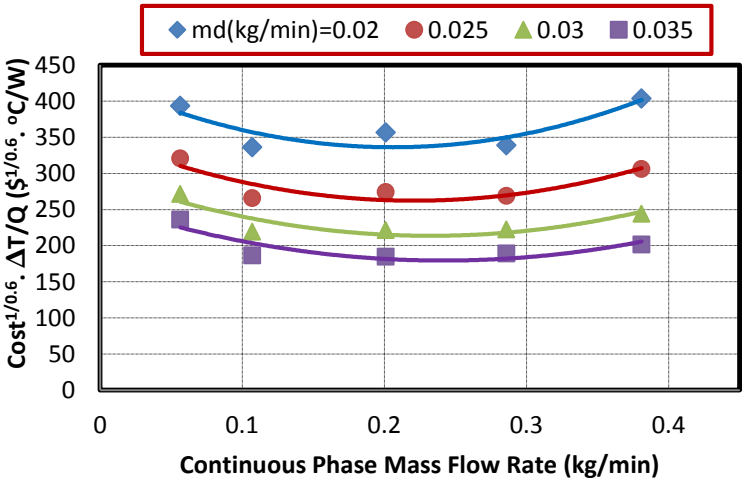

Fig. 10. Capital cost of three-phase direct contact condenser versus continuous mass flow rate for T_{di} = 40℃ and four different dispersed phase mass flow rates.

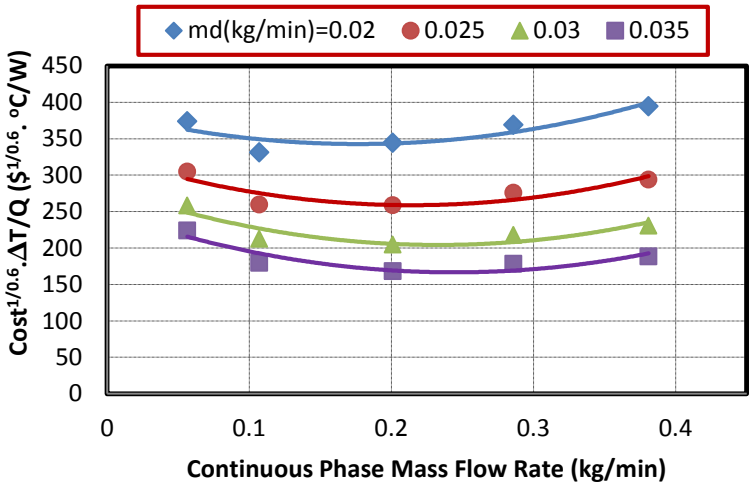

415

416 **Fig. 11.** Capital cost of three-phase direct contact condenser versus continuous mass flow rate

417 for $T_{di} = 43.5℃$ and four different dispersed phase mass flow rates.

418

419

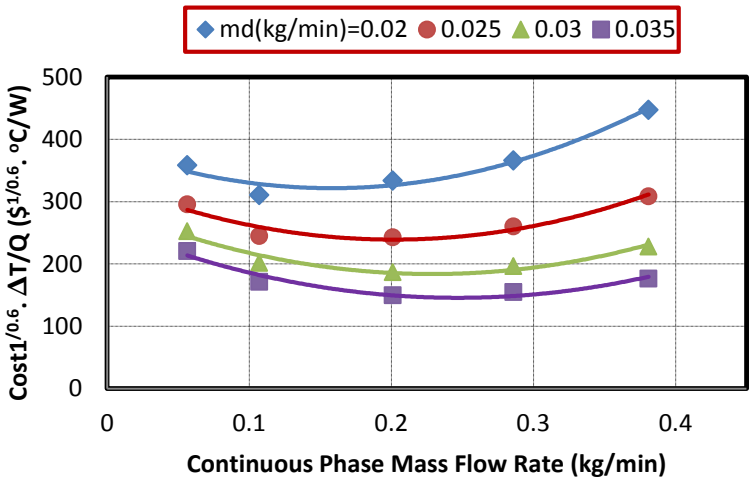

420

421 **Fig. 12.** Capital cost of three-phase direct contact condenser versus continuous mass flow rate

422 for $T_{di} = 47.5℃$ and four different dispersed phase mass flow rates.

423

424

425

426

427

To further show the economic advantages of the three-phase direct contact condenser, the ratio of the surface type (shell and tube condenser) to the three-phase direct contact condenser cost is calculated and shown in Fig. 13. It was found that this ratio increased with increasing dispersed phase mass flow rate. No significant impact of the continuous phase mass flow rate on the cost ratio can be identified from the figure. Only at very low continuous mass flow rates ($\dot{m}_c = 0.06\,\mathrm{kg/min}$) does the ratio seem a bit lower than at the other continuous phase mass flow rates, for an initial dispersed phase temperature 40℃. What is, once again, highlighted by this figure is that the very efficient heat transfer that is achieved in a direct contact condenser renders such a device considerably cheaper than the conventional equivalent. Fig 13 shows that there can be a difference of over an order of magnitude between the respective costs.

The effect of the initial temperature of the dispersed phase on the cost ratio is also evident from Fig. 13. Obviously, the effect of the initial dispersed phase temperature becomes more significant when the dispersed phase mass flow rate is higher. The initial temperature of the dispersed phase seems to have little effect at low to moderate dispersed phase mass flow rates ($\dot{m}_d \leq 0.025\,\mathrm{kg/min}$). It impact is more significant at a high dispersed phase mass flow rates ($\dot{m}_d > 0.025\,\mathrm{kg/min}$). In such cases, the higher the initial dispersed phase temperature, the higher the cost ratio. Nevertheless, this increase in the cost ratio, in total, seems confined to the effect of the dispersed phase mass flow rate.

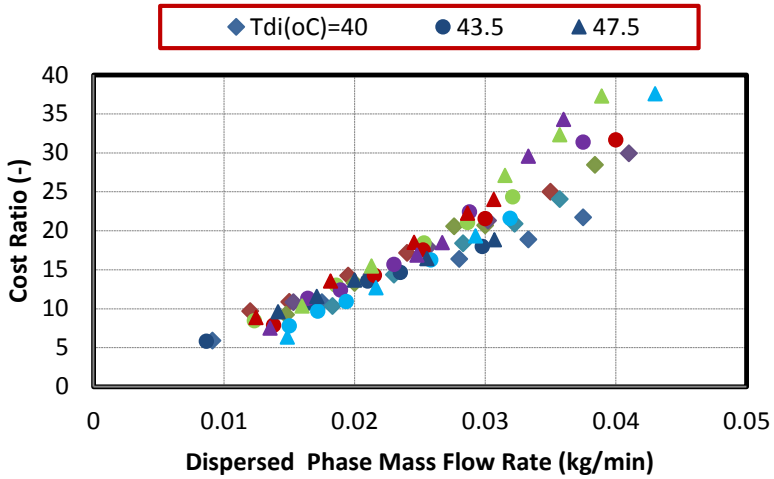

448

449 **Fig. 13.** Cost ratio versus dispersed mass flow rate for three different dispersed phase initial
450 temperatures ($T_{di} = 40℃,\ 43.5℃$ and $47.5℃$) and five different continuous phase mass
451 flow rates ($\dot{m}_c = 0.0564, 0.107, 0.201, 0.286$ and 0.381 kg/min) for each T_{di}.

452

453

454 The total heat transfer and the log-mean temperature difference are the parameters that can
455 most affect the capital cost estimate of the direct contact condenser. The calculation of these
456 parameters is strongly dependent on the different operational parameters of the condenser,
457 such as the continuous phase mass flow rate and the initial dispersed phase temperature.
458 Although an increase of the continuous phase mass flow rate results in an enhancement of the
459 direct contact condensation in the condenser, the increase in the total heat transfer is still
460 limited and constrained by the dispersed phase mass flow rate. At the same time, such a rise
461 in the total heat transfer might be balanced by an increase in the log-mean temperature
462 difference, which results from a high cooling rate. The results indicated (see sections above)
463 that there is no substantial effect of the initial temperature of the dispersed phase on the heat
464 transfer in the three-phase direct contact condenser, and consequently that latent heat is
465 dominant in such a process. As a result, the effect of these parameters on the capital cost
466 estimate of the direct contact condenser is less significant. This can be clearly demonstrated

by Figs. 14 and 15, which show that the capital cost index is largely independent of the initial temperature of the dispersed phase.

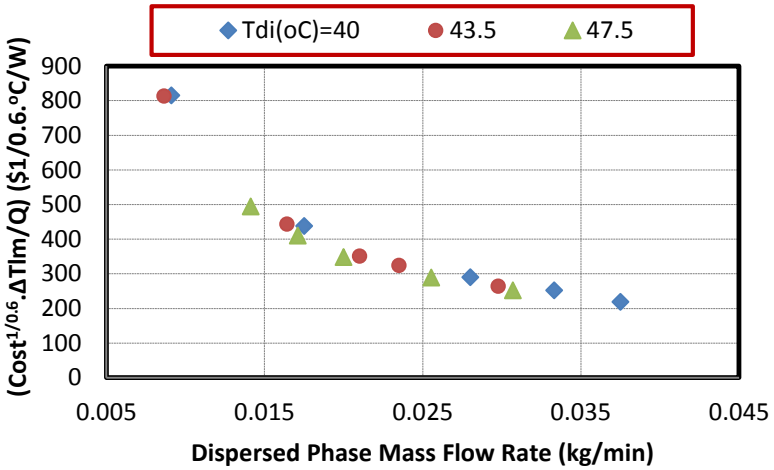

Fig. 14. Effect of dispersed phase initial temperature on the three-phase direct contact condenser capital cost for continuous phase mass flow rates ($\dot{m}_c = 0.0564$ kg/min).

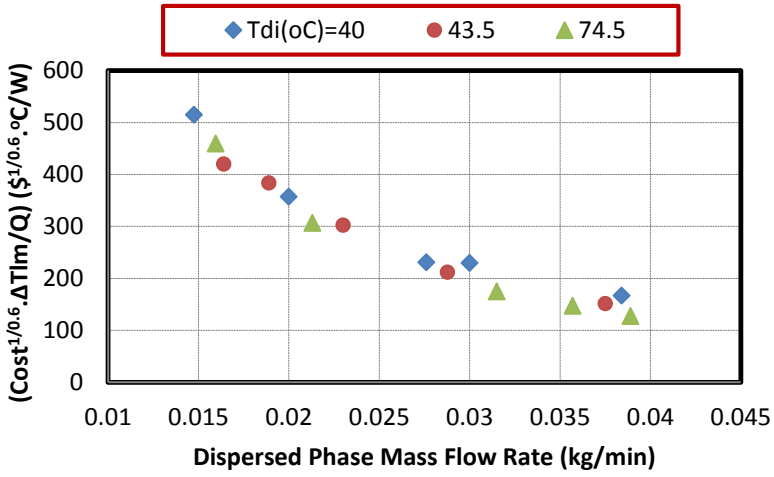

Fig. 15. Effect of dispersed phase initial temperature on the three-phase direct contact condenser capital cost for continuous phase mass flow rate ($\dot{m}_c = 0.201$ kg/min).

4. Conclusions

The efficiency and the capital cost of the three-phase direct contact condenser have been investigated experimentally. According to the experimental results, it is possible to conclude that the condenser's efficiency is significantly affected by the dispersed phase mass flow rate, less so by the continuous phase mass flow rate and only slightly affected by the dispersed phase initial temperature. Also, it was found that the condenser's capital cost is mainly affected by the dispersed phase mass flow rate. Very little effect of the continuous phase mass flow rate is shown in the results. An optimal value of the continuous phase mass flow rate at which the condenser's capital cost was at a minimum was evident. No notable effect of the dispersed phase initial temperature on the condenser's capital cost was observed.

Finally, the insights gained about the direct contact condenser's efficiency and capital cost suggest that it is useful to operate at relatively high continuous phase mass flow rate and high dispersed phase initial temperature. At these conditions, the efficiency of the condenser will be high; its capital cost will be a minimum. Furthermore, the operation will be far from the flooding limit of the column.

Nomenclture

A	area (m^2)
D	diameter (m)
C_A	cost of equpment of size A ($)
C_A	cost of equpment of size B ($)
F_c	total correction factor
F_m	correction factor based on condenser operational pressure

503 F_p correction factor based on the condenser material

504 H total condenser height (m)

505 H_o active condenser height (water level) (m)

506 I cost index

507 K_c constant appearing in Eq. (7)

508 M&*S* Marshall and Swift cost index

509 $\dot{m}_c$ continuous phase mass flow rate (kg/min)

510 $\dot{m}_d$ dispersed phase mass flow rate (kg/min)

511 R mass flow rate ratio

512 T temperature $(℃)$

513 ΔT_{lm} log-mean temperature difference $(℃)$

514 U overall heat transfer coefficient $(kJ/m^2 s\ K)$

515

516 **References**

517 [1] Chen Y. Novel cycles using carbon dioxide as working fluid. *Licenciate thesis, School of*
518 *Engineering and Management, Stockholm,* 2006

519 [2] Dizaji H, S, Jafarmadar S, Abbasalizadeh M, Khorasani S. Experiments on air bubbles
520 injection into a vertical shell and coiled tube heat exchanger; exergy and NTU analysis.
521 Energy Conv Mang (2015); 103:973-980.

522 [3] Rashidi S, Bovand M, Esfahani J, A. Heat transfer enhancement and pressure drop
523 penalty in porous solar heat exchangers: A sensitivity analysis. Energy Conv Mang
524 (2015); 103:726-738.

[4] Dammel F, Beer H. Heat transfer from a continuous liquid to an evaporating drop: a numerical analysis. Int J Therm Sci 2003; 4(7):677-686.

[5] Wanchoo R, Sharma S, Raina G. Drag coefficient and velocity of rise of a single collasping two-phase bubble. AIChE J 1997;4(8):1955-1963.

[6] Wanchoo R. Forced convection heat transfer around large two-phase bubbles condensing in an immiscible liquid. Heat Recovery Systems and CHP 1993; 13(5): 441-449.

[7] Gulevich A, Martynov P, Gulevsky V, Ulyanov V. Technologies for hydrogen production based on direct contact of gaseous hydrocarbons and evaporated water with molten Pb or Pb–Bi. Energy Conv Mang (2008); 49:1946-1950.

[8] Hewitt G, Shires G, Bott T. Process heat transfer, 1994, *CRC Publication, New York.*

[9] Vallario R, DeBellis D. State of technology of direct contact heat exchanging. 1984;84 NASA STI/Recon Technical Report N ,USA.

[10] Sideman S, Hirsch G. Direct contact heat transfer with change of phase: Condensation of single vapor bubbles in an immiscible liquid medium. Preliminary studies, AIChE J 1965;11(6):1019-1025.

[11] Isenberg J, Sideman S. Direct contact heat transfer with change of phase: bubble condensation in immiscible liquids. Int J Heat Mass Trans 1970;13(6):997-1011.

[12] Moalem D, Sideman S. The effect of motion on bubble collapse. Int J Heat Mass Trans 1973;16(12): 2321-2329.

[13] Higeta K, Mori Y, Komotori K. Condensation of a single vapor bubble rising in another immiscible liquid. in *AIChE Sym Ser*1979; 75 (189), San Diego: 256-265.

[14] Higeta K, Mori Y, Komotori K. A novel direct-contact condensation pattern of vapour bubbles in an immiscible liquid. The Canad J Chem Eng 1983; 61(6): 807-810.

548 [15] Lerner Y, Kalman H, Letan R. Condensation of an accelerating-decelerating bubble:
549 experimental and phenomenological analysis. J Heat Trans 1987;109(2): 509-517.

550 [16] Lerner Y, Letan R. Dynamics of condensing bubbles at intermediate frequencies of
551 injection. J Heat Trans 1990;112(3): 825-829.

552 [17] Kalman H, Mori Y. Experimental analysis of a single vapor bubble condensing in
553 subcooled liquid, Chem Eng J 2002;85(2): 197-206.

554 [18] Kalman H. Condensation of bubbles in miscible liquids. Int J Heat Mass Trans 2003;
555 46(18):3451-3463.

556 [19] Moalem D, Sideman S, Orell Hetsroni G. Direct contact heat transfer with change of
557 phase: condensation of a bubble train. Int J Heat Mass Trans 1973;16(12): 2305-2319.

558 [20] Kalman H. Condensation of a bubble train in immiscible liquids. Int J Heat Mass Trans
559 2006;49(13): 2391-2395.

560 [21] Mahood H B, Sharif A, Al-Ailbi S, Hossini A, Thorpe R B. Heat transfer modelling of
561 two-phase bubbles swarm condensing in three-phase direct-contact condenser. J Therm
562 Sci 2014; DOI: 10.2298/TSCI130219015M.

563 [22] Mahood H B, Campbell A N, Thorpe R B, Sharif A. A new model for the drag
564 coefficient of a swarm of condensing vapour–liquid bubbles in a third immiscible
565 liquid phase. Chem Eng Sci 2015;131:76-83.

566 [23] Sideman S, Moalem D. Direct contact heat exchangers: comparison of counter and co-
567 current condensers. Int J Multiphase Flow 1974;1(4):555-572.

568 [24] Mahood H B, Sharif A, Thorpe R B. Transient volumetric heat transfer coefficient
569 prediction of a three-phase direct contact condenser. J Heat Mass trans 2015;52(2):165-
570 170.

571 [25] Mahood H B, Sharif A, Al-Aibi S, Hawkins D, Thorpe R B. Analytical solution and
572 experimental measurements for temperature distribution prediction of three-phase
573 direct-contact condenser. Energy 2014; 67:538-547.

574 [26] Mahood H B, Thorpe R B, Campbell A N, Sharif A. Experimental measurements and
575 theoretical prediction for the transient characteristic of a three-phase direct contact
576 Condenser. Appl Them Eng 2015;87:161-174.

577 [27] Mahood H B, Thorpe R B, Campbell A N, Sharif A. Effect of various parameters on the
578 temperature measurements in a three-phase direct contact condenser. Int J Therm Tech
579 2015; 5(1) 23-27.

580 [28] Mahood H B, Campbell A N, Thorpe R B, Sharif A. Experimental measurements and
581 theoretical prediction for the volumetric heat transfer coefficient of a three-phase direct
582 contact condenser. Int Comm Heat Mass Trans 2015;66:180-188.

583 [29] Mahood H B, Sharif A, Thorpe R B, Campbell A N, Heat transfer measurements of a
584 three-phase direct contact condenser for application in energy production and water
585 desalination, 3rd Int. Conf. on Water, Energy and Environment, American University of
586 Sharjah, Sharjah, UAE, Paper-159, 24-27 March, 2015.

587 [30] Monning C, Numrich R. Condensation of vapours of immiscible liquids in the presence
588 of a non-condensable gas. Int J Therm Sci 1999;38:684e94.

589 [31] Farrington, R. B. and Wells, C. V., A thorough approach to measurement uncertainty
590 analysis applied to immersed heat exchanger testing, ASME Solar Energy Division
591 Conference, Anaheim, California, 14-17 April (1986).

592 [32] Guthrie K M. Data and techniques for preliminary capital cost estimating. Chem Eng
593 1969;76(6):114-126.

[33] Remer D S, Chai L H. Process Equipment, Cost Scale-up, *Encyclopedia of Chemical Processing and Design. Marcel Dekker, Inc., New York et al* 1993; 306-317.

[34] Ulrich G D. A guide to chemical engineering process design and economics, New York: John Wiley & Sons, Inc, 1984.